Biointerface Research in Applied Chemistry
Platinum Open Access Journal (ISSN: 2069-5837)

Article
Volume 12, Issue 3, 2022, 3790 - 3799
https://doi.org/10.33263/BRIAC123.37903799

Phytosynthesis of Iron Oxide Nanoparticles using *Juncus inflexus* Shoot Extract

Swetaleena Mishra [1,2], Jagannath Pradhan [1], Ravinder Singh [2], Brajesh Kumar [1,*]

[1] Department of Chemistry, TATA College, Kolhan University, Chaibasa-833202, Jharkhand, India
[2] University Department of Zoology, Kolhan University, Chaibasa-833202, Jharkhand, India
* Correspondence: krmbraj@gmail.com(B.K.);

Scopus Author ID 38961491900

Received: 6.04.2021; Revised: 15.05.2021; Accepted: 20.05.2021; Published: 13.08.2021

Abstract: To elude the toxic effects of chemically synthesized nanoparticles, the phytochemically synthesized nanoparticles may provide a better alternative. For the first time, an aqueous extract of *Juncus inflexus* shoot with $FeCl_3.6H_2O$ was used for the phytosynthesis of iron oxide nanoparticles (FeONPs). As-synthesized FeONPs were characterized by UV-Vis spectroscopy, Transmission electron microscopy (TEM), Dynamic light scattering (DLS), X-ray diffraction (XRD), and Fourier transform infrared spectroscopy (FTIR). FeONPs showed UV-vis absorption spectra between 300-400 nm, whereas TEM analysis confirmed the particle sizes of 40-60 nm with aggregation. XRD is confirming the polymorphic composition of Fe_3O_4, α-Fe_2O_3, and Fe^0 nanoparticles. Furthermore, FTIR analysis presenting the most probable mechanism for the synthesis of FeONPs. This multiphase FeONPs was applied for the decolorization of methylene blue dye (>83%). Phytosynthesized FeONPs have the benefits of low cost, no toxicity, sustainable, and eco-friendly technology so that they may be used as adsorbent/catalyst for remediation of toxic dyes in an aqueous medium.

Keywords: *Juncus inflexus*;iron oxide nanoparticles; green synthesis; TEM; adsorption.

1. Introduction

For the last few decades, Nanobiotechnology has enlightened a generous increase in the synthesis of materials of various types at the nanoscale level (1-100 nm) [1]. The importance of these materials was realized when researchers found that morphology can influence the physicochemical properties of substances due to the high surface-to-volume ratio, surface energy, spatial confinement, and reduced imperfections. Metal nanoparticles have distinctive physical, chemical, electronic, electrical, mechanical, magnetic, thermal, catalytic, dielectric, optical, and biological properties in contrast to bulk materials [2]. Iron oxide nanoparticles (FeONPs) exist with different polymorph (α-Fe_2O_3, γ-Fe_2O_3, Fe_3O_4, and FeO) structures [3]. Among all other metal nanoparticles, FeONPs have widely studied the material and possess tremendous applications as photocatalysts, sensors, fine ceramics, plant growth regulators, water purification, medical applications, data storage materials, pigments, anticorrosive agents [4], and photoelectrochemical cells [5].

To date, many strategies have been employed to synthesize the FeONPs with different morphology and purity. The building up approach to synthesize FeONPs includes various physical and chemical methods as hydrothermal synthesis [6], co-precipitation [7], ultrasound-assisted synthesis [8], microwave-assisted synthesis [9], microemulsion [10], and γ-irradiation synthesis [11] are well known. Between these various methods, successful green chemistry

preparation of FeONPs via phytochemical/ plant extract as reducing and stabilizing agents is an alternative co-precipitation method, owing to its simplicity, economically viable, eco-friendly, biocompatible, safe, and cost-effective [12, 13]. It includes phytosynthesis of FeONPs using aqueous extract of *Amaranthus dubius* [14], *Dodonaea viscosa* [15], Andean blackberry [16], *Ruellia tuberosa* [17], Omani mango [18], *Peltophorum pterocarpum* [19], *Laurus nobilis* [20], *Daphne mezereum* [21], *Cucurbita moschata* [22], and *Moringa oleifera* leaves [23], *Beta vulgaris* stalks [22], *Syzygium aromaticum* buds [24], *Citrus paradisi* [3], Korla fragrant [25], and *Punica granatum* rind [26], *Cornus mas*[5], *Withania coagulans*[26], *Passiflora tripartita* [27] and *Ficus carica* fruit [28], Fenugreek [7] and *Punica granatum* seed [30], *Avicennia marina* [31] and *Hibiscus rosa-sinensis* flower [32].

Juncus inflexus plant is among the most common and valuable fiber plants that belongs to the Juncaceae family and is distributed worldwide. They are epiphyte that appears like long grass and commonly referred to as the rushes. This plant is used to produce traditional mats, baskets, and other craftwork items [33]. Its shoot contains several groups of natural compounds, including flavonoids, coumarins, terpenes, sterols, phenolic acids, lignin, stilbenes, dihydro-dibenzoxepin, carotenoids, and phenanthrenes (monomeric and dimeric) [34].

Based on the aforementioned facts, this work describes, for the first time, the phytosynthesis of FeONPs by using an aqueous extract of Juncus inflexus shoot with $FeCl_3.6H_2O$ and characterized by UV-Vis spectroscopy, Transmission electron microscopy (TEM), Dynamic light scattering (DLS), X-ray diffraction (XRD) and Fourier transform infrared spectroscopy (FTIR). Schematic representation for green synthesis of FeONPs using Juncus inflexus shoot extract is shown in Figure 1. These nanoparticles were further used as adsorbent/ catalyst in a preliminary application to remove harmful cationic dye, methylene blue (MB), in an aqueous medium.

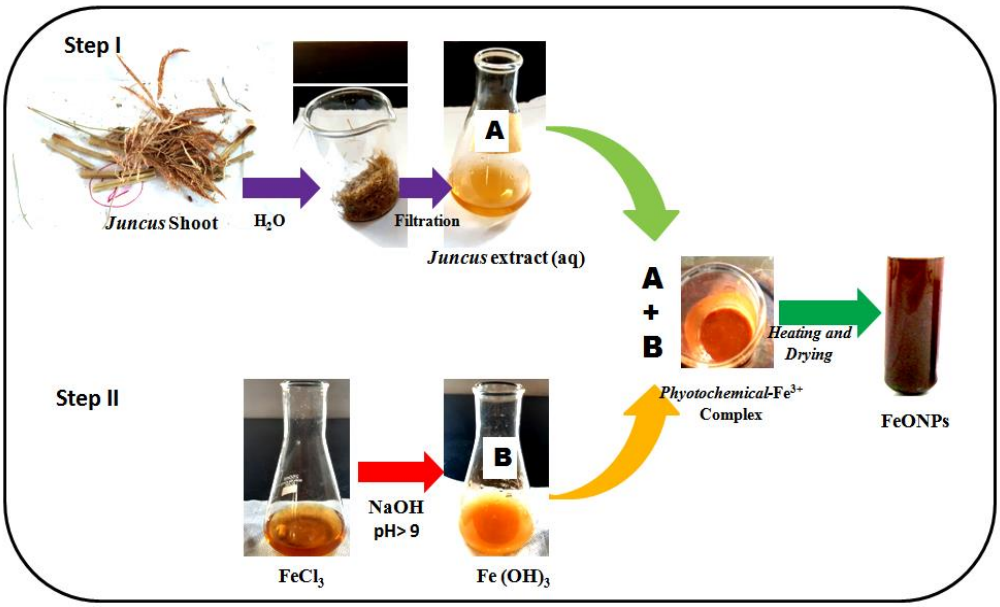

Figure 1. Schematic representations for green synthesis of FeONPs using *Juncus inflexus* shoot extract.

2. Materials and Methods

2.1. Materials.

Analytical grade $FeCl_3.6H_2O$ (99.0 %)and methylene blue (MB, 98.5%), and NaOH were purchased from BDH Chemicals, India. Ultrapure water was used for the preparation of

all solutions. *Juncus inflexus* plants were collected on 18th December 2018 from the riverside of Subarnarekha River, Mau Bhandar, Jharkhand, India.

2.2. Extraction of phytochemicals from Juncus inflexus.

The collected plant was shade dried for 3 weeks and crushed into small pieces using a motor and pestle. 1 g of dried *Juncus inflexus* shoot powder was added to 50 mL distilled water containing 2 mL ethanol; heated (80-90°C) for 20 min. After cooling, the yellowish color *J. inflexus* extract was filtered using Whatman paper no.1 and maintain its volume up to 100 mL using water in 100 mL Erlenmeyer flask and stored at 4 °C for further use.

2.3. General procedure for the synthesis of FeONPs.

In a typical reaction procedure, 3–4 mL of Juncus shoot extract was added to 20 mL containing $FeCl_3$ (10 mM), and pH is adjusted >9, using 5% NaOH solution, then the solution was placed under vigorous magnetic stirring for 60 mins at 80 °C till the brownish-black color solution completely replaced yellowish red color, indicated the formation of FeONPs. The resulting iron oxide nanoparticle was centrifuged thrice at 5000 rpm for 10 min and washed several times with water: ethanol (1:1) mixtures. The purified nanoparticles powder was dried at 80 °C for 48 h and then stored in an airtight bottle for further analytical characterization.

2.4. Adsorption activity.

In order to evaluate the adsorption ability of FeONPs, MB dye was used for a model experiment under atmospheric pressure in single-use at 23-25 °C was performed. 50 mg FeONPs was mixed with 10 mL of MB (20 mg/L) in a glass tube at pH 6 and kept at room temperature after vortexed for 10 sec. Then, the sample containing a glass tube was properly capped and shaken at 120 rpm. The progress of the adsorption of dye on the surface of FeONPs was monitored by measuring the absorption of MB in the filtrate at the wavelength 664 nm, using a UV–vis absorption spectrometer, and the adsorption percentage of MB was calculated using Eq. (1).

$$\eta = (A_0\text{-}A_t)/A_0 \times 100\% \quad (1)$$

where η is the rate of removal of MB in terms of %, A_0 is the initial absorbance of the dye solution, and A_t is the absorbance of the MB at time t. [3]

2.5. Analytical characterization of FeONPs.

The optical properties of samples containing extracts and FeONPs were confirmed by UV- visible, single beam spectrophotometer (LABMAN, China) and graph plotted on the Origin 6.1 program. The hydrodynamic size distribution of FeONPs was analyzed in a dynamic light scattering (DLS) instrumentation from HORIBA, Japan. Morphology and selected area electron diffraction (SAED) pattern of as-synthesized FeONPs were determined using transmission electron microscopy (TEM) by FEI Tecnai. X-ray Diffraction (XRD) analyses on thin films of the nanoparticles were carried out using a BRUKER D8 ADVANCE brand θ-2θ configuration (generator-detector) X-ray tube copper λ = 1.54 A and LYNXEYE PSD detector. The FTIR-ATR spectra were collected in the transmission mode (4000–650 cm^{-1}) using a Perkin Elmer spectrophotometer (Model RZX). The pH measurements of the metal ion solution were done by using a pH meter.

3. Results and Discussion

3.1. UV-Vis and Visual analysis.

UV–Vis absorption spectra of an aqueous solution of the *J. inflexus* shoot extract were observed in the absence and presence of Fe^{3+} ions (Figure 2). It was found that the absorbance of *J. inflexus* extract is altered significantly and interacts with the Fe^{3+} ion, and confirmed the formation of FeONPs. The absorbance of the reaction solution decreased in the range of 300-400 nm with respect to *J. inflexus* shoot extract, whereas the absorbance peak around 300-550 nm of $FeCl_3$ was also disappeared. It may be due to the involvement of bio-molecules like polyphenols and lignin-containing hydroxyl, carboxylic and carbonyl groups of *J. inflexus* for the synthesis of nanoparticles ($E°_{red}$ of flavonoids/polyphenolic = 0.3–0.8 V whereas, the $E°_{red}$ of Fe^{3+} to Fe^{2+} and Fe^{2+} to Fe is just 0.77 V and – 0.44 V) [17]. The visual color change from yellow plant extract into dark brown or brownish-black (Inset: Figure 2a-c) and their absorption peak confirmed the formation of spherical or pseudo spherical FeONPs and consistent with the earlier report [3, 14, 15, 29].

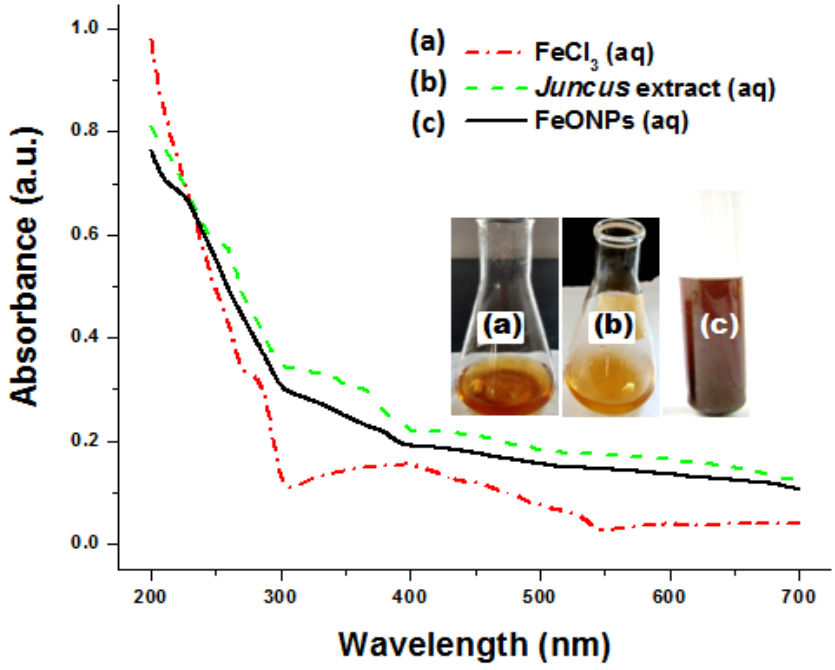

Figure 2. UV-Vis and visual analysis of (**a**) $FeCl_3$, (**b**) *Juncus inflexus* shoot extract, and (**c**) as-prepared FeONPs.

3.2. TEM, SAED and DLS analysis.

TEM is based on the electron transmittance principle so that it can provide information on the different morphologies and layering of material from very low to higher magnification. TEM micrograph of FeONPs synthesized using *J. inflexus* has shown in Figure 3. It was found that the FeONPs were prepared by *J. inflexus* spherical in shape and size ranges from 40-60 nm. All nanoparticles were surrounded by *J. inflexus* extract. Due to the magnetic nature of iron, most of the FeONPs were aggregated. SAED image (Figure 3b1) confirmed the semi-crystalline and spherical nature of as-synthesized FeONPs [3, 15]. The hydrodynamic size distribution of FeONPs was determined by the DLS method (Figure 4). It reveals the formation of FeONPs having an average particle diameter of 196.5± 72.9 nm with a polydispersity index (PDI) = 0.1367. PDI > 0.1, clearly indicates that as-synthesized FeONPs were polydispersed.

The obtained size in DLS differs from TEM images either due to the aggregation of FeONPs by forming a thin layer of phytochemicals surrounding the nanoparticles or screening smaller nanoparticles by bigger particles [3, 28].

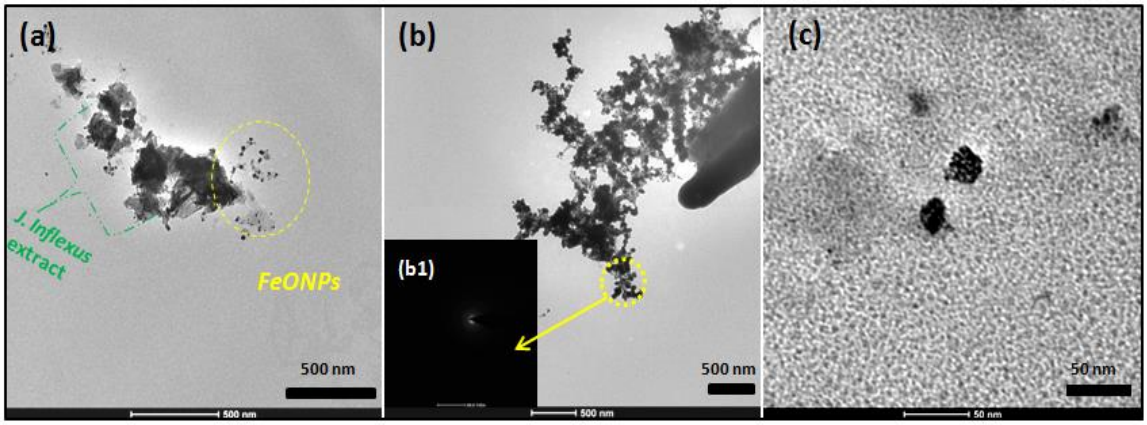

Figure 3. (a, b, c) TEM images and (b1) SAED pattern of as-prepared FeONPsusing *J. influxes* shoot extract.

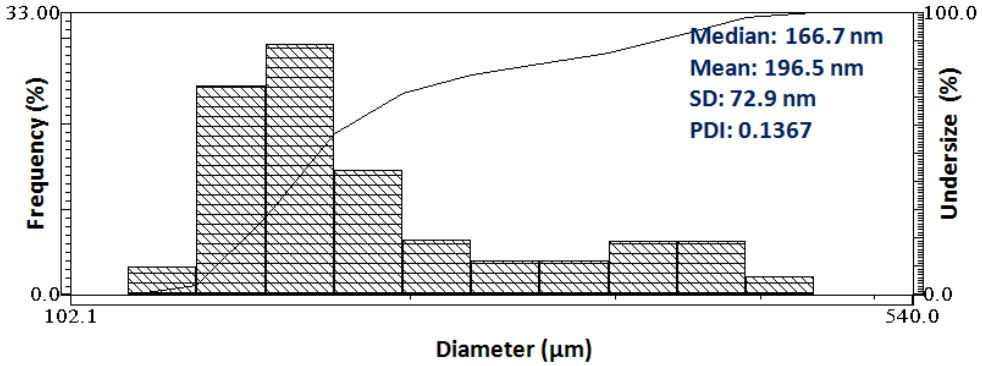

Figure 4. DLS size distribution pattern of as-prepared FeONPs using *J. inflexus* shoot extract.

3.3. XRD and FTIR analysis.

XRD reveals the structural properties of nanoparticles. Figure 5 shows the XRD diffraction pattern of as-prepared FeONPs obtained from *J.inflexus* shoot extract. It confirms that as-prepared FeONPs nanoparticles are polymorphic composition and containing a mixture of Fe_3O_4 and α-Fe_2O_3. On comparing with ICSD No: 01-088-2324, a very small amount, 3.5% of Fe (0), are also present. The 2θ peaks are indexed as 111 and 220 to the crystal planes of Fe_3O_4 [16, 17, 24, 26], whereas 012 and 113 are attributed for α-Fe_2O_3 [3, 24, 30], respectively. The interactions between Fe^{3+} ions precursor and extracts *J. inflexus* extract were hypothesized by FTIR spectrum analysis. FTIR spectrum of *J. inflexus*extract capped FeONPswas is shown in Figure 6.The absorption peak at 3320 cm^{-1} corresponds to O–H stretching vibrations, a feature of alcohols and phenols [30] whereas, a weak absorption peak at 2927 cm^{-1} is attributed to C-H aliphatic vibrations of *J. inflexus* phytochemicals (cellulose and hemicellulose) coated FeONPs [30, 33-36]. The strong peak at 1601 cm^{-1} signifies the presence of a strong C=O/ C=N bond resulting from stretching vibrational mode in the lignin-coated FeONPs. Other peaks at 1396 and 1044 cm^{-1} indicate the existence of C-H bending and C-OH/ C-O-C stretching vibration of the phenolic group and cellulose backbone [3, 24]. These absorption peaks are slightly different from the earlier reported FTIR peaks of *Juncus*. The FTIR analysis helped identify bio-molecules like flavonoids, coumarins, terpenes, sterols, phenolic acids, lignin, etc., which involved the synthesis and stabilization of FeONPs. The hydrophilicity of *J. inflexus* phytochemicals (-COOH, -C-OH, $-NH_2$) can bound the surface of the nanoparticles via H-

bonding and causing aggregation [13, 34, 36]. The obtained FTIR result is in agreement with the UV-Visible, TEM, and DLS results.

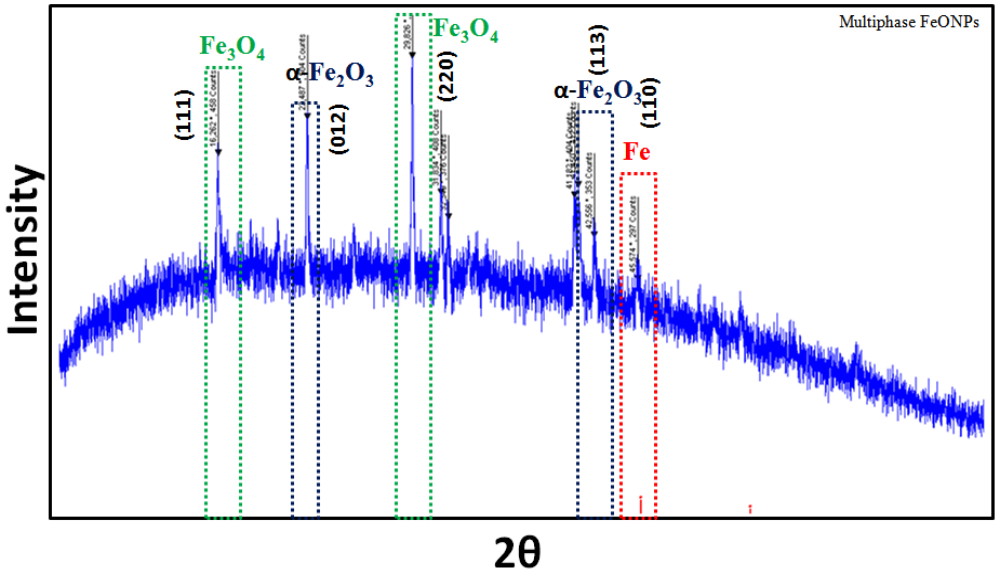

Figure 5. XRD pattern of as-prepared FeONPs using *J. inflexus* shoot extract.

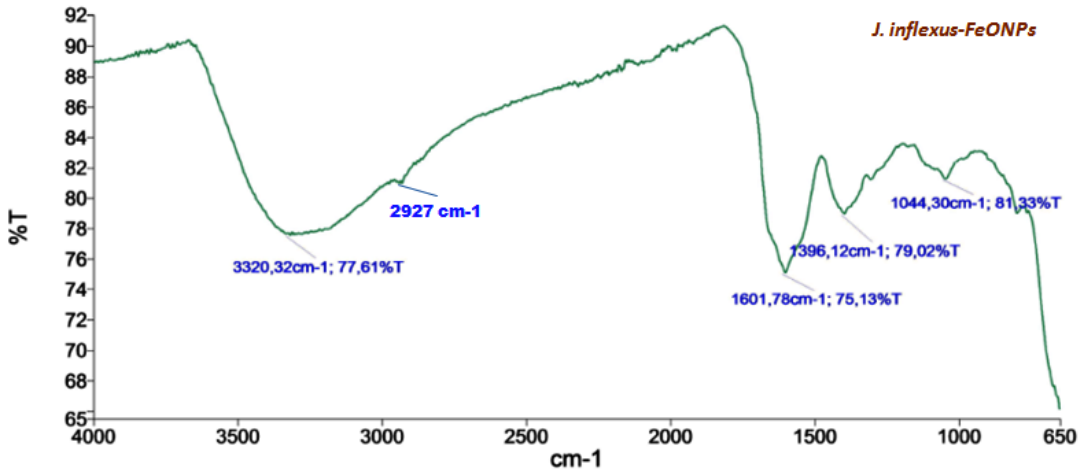

Figure 6. FTIR spectrum of FeONPs prepared by *J. inflexus* shoot extract.

3.4 Adsorption of MB on the surface of FeONPs and its suggested mechanism.

As a well-known separation process, adsorption has been widely applied to remove chemical pollutants from wastewater due to its simplicity, cost-effectiveness and insensitivity to pollutants. Therefore, FeONPs are currently being explored as an effective and low-cost adsorbent with high adsorption capacity for organic pollutant removal. A strong external magnetic field is more recommended [37]. Figure 7 shows the initial screening of the adsorption/degradation of MB from aqueous synthetic solutions by using *J. inflexus*-FeONPs. As shown in Figure 7, the adsorption activity of as-synthesized FeONPs increases with the increase of contact time. The amount of MB removed was increased steadily by decreasing intensity at 664 nm corresponding to the n–π* transition of MB. The decolorization capacities for FeONPs were reached within 120 mins. MB is a thiazine-based blue color cationic dye that is used as an anti-malarial, chemotherapeutic agent, colorant in the textile industry, and sulfide ions analysis [38]. Excessive MB in water bodies is toxic and toxic and can be harmful to human health, creating difficulties in breathing, vomiting, diarrhea, and nausea [16, 39]. The removal efficiency rate (η) of MB was 67.33 and 83.06 % for 60 and 120 mins. It can be seen

that the color of MB drastically faded to colorless after 120 mins at the natural pH (Figure 7, Inset).

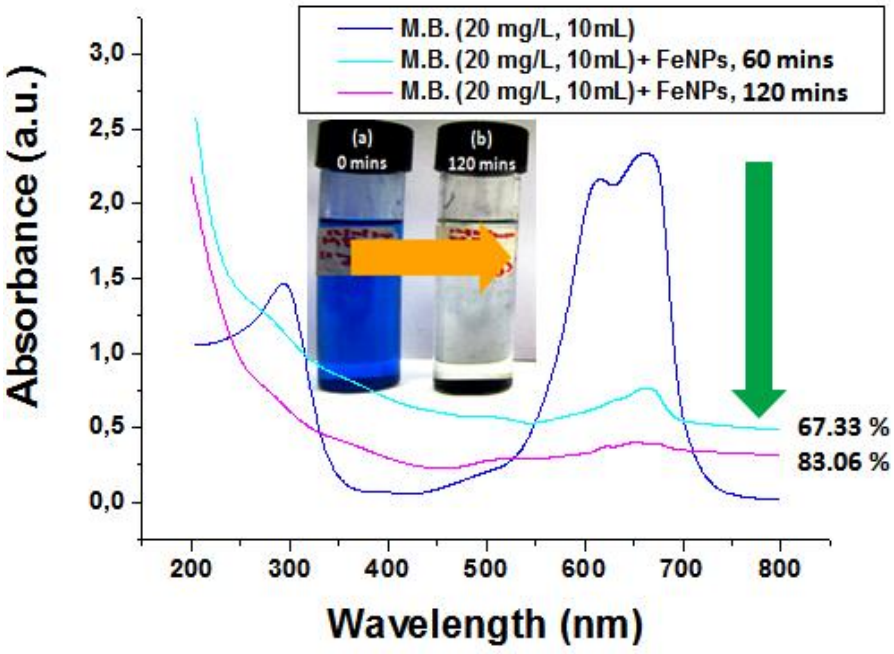

Figure 7. Adsorption of MB dye using 50 mg of as-prepared FeONPs for 60 and 120 mins (Inset: It shows a visual picture of MB before and after addition of FeONPs for 120 mins).

Surface complexation via electrostatic interaction has been demonstrated as the dominant mechanism for the sorption of organic acids on metal oxide surfaces under most solution conditions [38, 40].

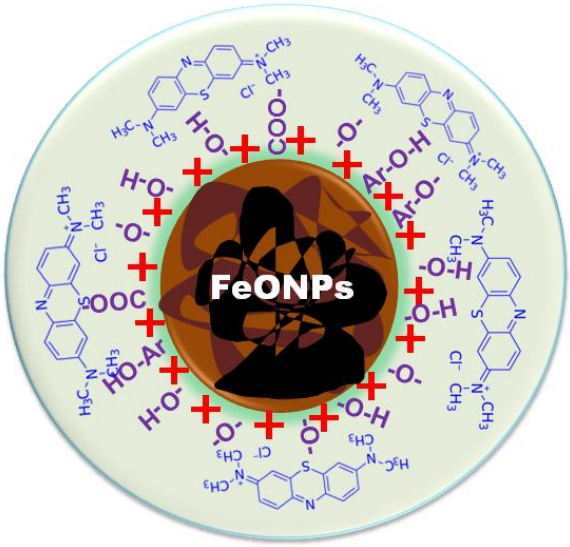

Figure 8. Suggested mechanism for adsorption of MB dye on the surface of as-prepared Fe-ONPs.

This study suggested the adsorption of the MB containing the $–NR_2$ on the surface of FeONPs. At normal pH values 6~7, there are fewer hydrogen ions to compete with the cationic dye pollutants for the adsorption sites of FeONPs. Indeed, a high concentration of -OH, $-COO^-$, and negative charges surface of the nanoparticles (Figure 8) enhancing the attraction and adsorption of cationic dyes; thus, increasing the removal efficiency [41]. Similar adsorption activity has been reported by Kumar *et al.*, 2020 [3] and Cheera *et al.*, 2016 [42] for green synthesized FeONPs from peel extracts of *Citrus paradisi*, and *Ridge gourd*, which caused

80% and 96 % degradation of MB dye. The removal efficiency of cationic dyes on the surface of FeONPs was enhanced at normal pH. Further work will be needed to optimize the MB decolorization procedure using different metallic nanoparticles. This process is of great industrial interest, and the use of agricultural waste in nanoscience offers a sustainable and eco-friendly approach for wastewater treatment.

4. Conclusions

This report demonstrated that multiple phase FeONPs can be obtained from $FeCl_3.6H_2O$ in the presence of *J.inflexus* extract via the green synthesis route. The obtained FeONPs are spherical in shape with sizes 40-60 nm. The phytosynthesized FeONPs were characterized by UV-Vis spectroscopy, TEM, DLS, XRD and FTIR techniques. As-synthesized FeONPs displayed potential degradation activity against the MB dye (~83%). The method may be scalable for industrial production since it needs widely available *J.inflexus* and lacks any special condition for reactant addition. The benefit of nanoremediation, using green synthesized FeONPs, can favor the cost-effective and eco-friendly decontaminate of toxic dyes on a large scale.

Funding

This scientific work has been funded by TATA College, India.

Acknowledgments

This scientific work has been funded by TATA College, India.

Conflicts of Interest

The authors confirm they have no conflict of interest.

References

1. Deokar, G.K.; Ingale, A.G. Green synthesis of gold nanoparticles (Elixir of Life) from banana fruit waste extract – an efficient multifunctional agent. *RSC Advances* **2016**, *6*, 74620-74629, https://doi.org/10.1039/C6RA14567A.
2. Daniel, M.-C.; Astruc, D. Gold Nanoparticles: Assembly, Supramolecular Chemistry, Quantum-Size-Related Properties, and Applications toward Biology, Catalysis, and Nanotechnology. *Chem. Rev.* **2004**, *104*, 293-346, https://doi.org/10.1021/cr030698+.
3. Kumar, B.; Smita, K.; Galeas, S.; Sharma, V.; Guerrero, V.H.; Debut, A.; Cumbal, L. Characterization and application of biosynthesized iron oxide nanoparticles using *Citrus paradisi* peel: A sustainable approach. *Inorg. Chem. Commun.* **2020**, *119*, 108116, https://doi.org/10.1016/j.inoche.2020.108116.
4. Ene,V. L.; Neacsu, I. A.; Oprea, O.; Surdu, V. A.; Trusca, R. D.; Ficai, A.; Andronescu, E. Single Step Synthesis of glutamic/tartaric acid-stabilised Fe_3O_4 nanoparticles for targeted delivery systems. *Revista de Chimie*, **2020**, 71, 230-238, https://doi.org/10.37358/RC.20.2.7920.
5. Rostamizadeh, E.; Iranbakhsh, A.; Majd, A.; Arbabian, S.; Mehregan, I. Green synthesis of Fe_2O_3 nanoparticles using fruit extract of Cornus mas L. and its growth-promoting roles in Barley. *Journal of Nanostructure in Chemistry* **2020**, *10*, 125-130, https://doi.org/10.1007/s40097-020-00335-z.
6. Fan, R.; Chen, X.H.; Gui, Z.; Liu, L.; Chen, Z.Y. A new simple hydrothermal preparation of nanocrystalline magnetite Fe_3O_4. *Mater. Res. Bull.* **2001**, *36*, 497-502, https://doi.org/10.1016/S0025-5408(01)00527-X.
7. Roth, H.-C.; Schwaminger, S.P.; Schindler, M.; Wagner, F.E.; Berensmeier, S. Influencing factors in the CO-precipitation process of superparamagnetic iron oxide nano particles: A model based study. *J. Magn. Magn. Mater*. **2015**, *377*, 81-89, https://doi.org/10.1016/j.jmmm.2014.10.074.

8. Deshmukh, A.R.; Gupta, A.; Kim, B.S. Ultrasound assisted green synthesis of silver and iron oxide nanoparticles using fenugreek seed extract and their enhanced antibacterial and antioxidant activities. *BioMed Research International* **2019**, *2019*, 1714358, https://doi.org/10.1155/2019/1714358.
9. Lastovina, T.A.; Budnyk, A.P.; Kubrin, S.P.; Soldatov, A.V. Microwave-assisted synthesis of ultra-small iron oxide nanoparticles for biomedicine. *Mendeleev Commun.* **2018**, *28*, 167-169, https://doi.org/10.1016/j.mencom.2018.03.019.
10. Li, Y.; Jiang, R.; Liu, T.; Lv, H.; Zhou, L.; Zhang, X. One-pot synthesis of grass-like Fe_3O_4 nanostructures by a novel microemulsion-assisted solvothermal method. *Ceram. Int.* **2014**, *40*, 1059-1063, https://doi.org/10.1016/j.ceramint.2013.06.104.
11. Jurkin, T.; Gotić, M.; Štefanić, G.; Pucić, I. Gamma-irradiation synthesis of iron oxide nanoparticles in the presence of PEO, PVP or CTAB. *Radiat. Phys. Chem.* **2016**, *124*, 75-83, https://doi.org/10.1016/j.radphyschem.2015.11.019.
12. Fahmy, H.M.; Mohamed, F.M.; Marzouq, M.H.; Mustafa, A.B.E.-D.; Alsoudi, A.M.; Ali, O.A.; Mohamed, M.A.; Mahmoud, F.A. Review of Green Methods of Iron Nanoparticles Synthesis and Applications. *BioNanoScience* **2018**, *8*, 491-503, https://doi.org/10.1007/s12668-018-0516-5.
13. Sadhasivam, S.; Vinayagam, V.; Balasubramaniyan, M. Recent advancement in biogenic synthesis of iron nanoparticles. *J. Mol. Struct.* **2020**, *1217*, 128372,https://doi.org/10.1016/j.molstruc.2020.128372.
14. Harshiny, M.; Iswarya, C.N.; Matheswaran, M. Biogenic synthesis of iron nanoparticles using Amaranthus dubius leaf extract as a reducing agent. *Powder Technol.* **2015**, *286*, 744-749, https://doi.org/10.1016/j.powtec.2015.09.021.
15. Kiruba Daniel, S.C.G.; Vinothini, G.; Subramanian, N.; Nehru, K.; Sivakumar, M. Biosynthesis of Cu, ZVI, and Ag nanoparticles using *Dodonaea viscosa* extract for antibacterial activity against human pathogens. *J. Nanopart. Res.* **2012**, *15*, 1319, https://doi.org/10.1007/s11051-012-1319-1.
16. Kumar, B.; Smita, K.; Cumbal, L.; Debut, A.; Galeas, S.; Guerrero, V.H. Phytosynthesis and photocatalytic activity of magnetite (Fe_3O_4) nanoparticles using the Andean blackberry leaf. *Mater. Chem. Phys.* **2016**, *179*, 310-315, https://doi.org/10.1016/j.matchemphys.2016.05.045.
17. Vasantharaj, S.; Sathiyavimal, S.; Senthilkumar, P.; LewisOscar, F.; Pugazhendhi, A. Biosynthesis of iron oxide nanoparticles using leaf extract of *Ruellia tuberosa*: Antimicrobial properties and their applications in photocatalytic degradation. *J. Photochem. Photobiol. B: Biol.* **2019**, *192*, 74-82, https://doi.org/10.1016/j.jphotobiol.2018.12.025.
18. Al-Ruqeishi, M.S.; Mohiuddin, T.; Al-Saadi, L.K. Green synthesis of iron oxide nanorods from deciduous Omani mango tree leaves for heavy oil viscosity treatment. *Arabian Journal of Chemistry* **2019**, *12*, 4084-4090, https://doi.org/10.1016/j.arabjc.2016.04.003.
19. Anchan, S.; Pai, S.; Sridevi, H.; Varadavenkatesan, T.; Vinayagam, R.; Selvaraj, R. Biogenic synthesis of ferric oxide nanoparticles using the leaf extract of *Peltophorum pterocarpum* and their catalytic dye degradation potential. *Biocatalysis and Agricultural Biotechnology* **2019**, *20*, 101251, https://doi.org/10.1016/j.bcab.2019.101251.
20. Jamzad, M.; Kamari Bidkorpeh, M. Green synthesis of iron oxide nanoparticles by the aqueous extract of *Laurus nobilis* L. leaves and evaluation of the antimicrobial activity. *Journal of Nanostructure in Chemistry* **2020**, *10*, 193-201, https://doi.org/10.1007/s40097-020-00341-1.
21. Beheshtkhoo, N.; Kouhbanani, M.A.J.; Savardashtaki, A.; Amani, A.M.; Taghizadeh, S. Green synthesis of iron oxide nanoparticles by aqueous leaf extract of *Daphne mezereum* as a novel dye removing material. *Appl. Phys. A* **2018**, *124*, 363, https://doi.org/10.1007/s00339-018-1782-3.
22. de Lima Barizão, A.C.; Silva, M.F.; Andrade, M.; Brito, F.C.; Gomes, R.G.; Bergamasco, R. Green synthesis of iron oxide nanoparticles for tartrazine and bordeaux red dye removal. *Journal of Environmental Chemical Engineering* **2020**, *8*, 103618, https://doi.org/10.1016/j.jece.2019.103618.
23. Aisida, S.O.; Madubuonu, N.; Alnasir, M.H.; Ahmad, I.; Botha, S.; Maaza, M.; Ezema, F.I. Biogenic synthesis of iron oxide nanorods using *Moringa oleifera* leaf extract for antibacterial applications. *Applied Nanoscience* **2020**, *10*, 305-315, https://doi.org/10.1007/s13204-019-01099-x.
24. T, S.J.K.; V.R, A.; M, V.; Muthu, A. Biosynthesis of multiphase iron nanoparticles using *Syzygium aromaticum* and their magnetic properties. *Colloids Surf. Physicochem. Eng. Aspects* **2020**, *603*, 125241, https://doi.org/10.1016/j.colsurfa.2020.125241.
25. Rong, K.; Wang, J.; Zhang, Z.; Zhang, J. Green synthesis of iron nanoparticles using Korla fragrant pear peel extracts for the removal of aqueous Cr(VI). *Ecol. Eng.* **2020**, *149*, 105793, https://doi.org/10.1016/j.ecoleng.2020.105793.

26. Venkateswarlu, S.; Kumar, B.N.; Prathima, B.; SubbaRao, Y.; Jyothi, N.V.V. A novel green synthesis of Fe3O4 magnetic nanorods using *Punica Granatum* rind extract and its application for removal of Pb(II) from aqueous environment. *Arabian Journal of Chemistry* **2019**, *12*, 588-596, https://doi.org/10.1016/j.arabjc.2014.09.006.
27. Qasim, S.; Zafar, A.; Saif, M.S.; Ali, Z.; Nazar, M.; Waqas, M.; Haq, A.U.; Tariq, T.; Hassan, S.G.; Iqbal, F.; Shu, X.-G.; Hasan, M. Green synthesis of iron oxide nanorods using *Withania coagulans* extract improved photocatalytic degradation and antimicrobial activity. *J. Photochem. Photobiol. B: Biol.* **2020**, *204*, 111784, https://doi.org/10.1016/j.jphotobiol.2020.111784.
28. Kumar, B.; Smita, K.; Cumbal, L.; Debut, A. Biogenic synthesis of iron oxide nanoparticles for 2-arylbenzimidazole fabrication. *Journal of Saudi Chemical Society* **2014**, *18*, 364-369, https://doi.org/10.1016/j.jscs.2014.01.003.
29. Kumar, B.; Smita, K.; Galeas, S.; Guerrero, V.H.; Debut, A.; Cumbal, L. One-Pot Biosynthesis of Maghemite (γ-Fe2O3) Nanoparticles in Aqueous Extract of *Ficus carica* Fruit and Their Application for Antioxidant and 4-Nitrophenol Reduction. *Waste and Biomass Valorization* **2020**, https://doi.org/10.1007/s12649-020-01279-9.
30. Bibi, I.; Nazar, N.; Ata, S.; Sultan, M.; Ali, A.; Abbas, A.; Jilani, K.; Kamal, S.; Sarim, F.M.; Khan, M.I.; Jalal, F.; Iqbal, M. Green synthesis of iron oxide nanoparticles using pomegranate seeds extract and photocatalytic activity evaluation for the degradation of textile dye. *Journal of Materials Research and Technology* **2019**, *8*, 6115-6124, https://doi.org/10.1016/j.jmrt.2019.10.006.
31. Karpagavinayagam, P.; Vedhi, C. Green synthesis of iron oxide nanoparticles using *Avicennia marina* flower extract. *Vacuum* **2019**, *160*, 286-292, https://doi.org/10.1016/j.vacuum.2018.11.043.
32. Razack, S.A.; Suresh, A.; Sriram, S.; Ramakrishnan, G.; Sadanandham, S.; Veerasamy, M.; Nagalamadaka, R.B.; Sahadevan, R. Green synthesis of iron oxide nanoparticles using *Hibiscus rosa-sinensis* for fortifying wheat biscuits. *SN Applied Sciences* **2020**, *2*, 898, https://doi.org/10.1007/s42452-020-2477-x.
33 Naili, H.; Jelidi, A.; Limam, O.; Khiari, R. Extraction process optimization of *Juncus* plant fibers for its use in a green composite. *Industrial Crops and Products* **2017**, *107*, 172-183, https://doi.org/10.1016/j.indcrop.2017.05.006.
34. Park, S.; Yang, S.; Ahn, D.; Yang, J.H.; Kim, D.K. Antioxidative phenolic compounds from the whole plant of *Juncus diastrophanthus*. *Journal of the Korean Society for Applied Biological Chemistry* **2011**, *54*, 685-692, https://doi.org/10.1007/BF03253146.
35. Xia, L.; Zhang, C.; Wang, A.; Wang, Y.; Xu, W. Morphologies and properties of Juncus effusus fiber after alkali treatment. *Cellulose* **2020**, *27*, 1909-1920, https://doi.org/10.1007/s10570-019-02933-9.
36. Bhuiyan, M.S.H.; Miah, M.Y.; Paul, S.C.; Aka, T.D.; Saha, O.; Rahaman, M.M.; Sharif, M.J.I.; Habiba, O.; Ashaduzzaman, M. Green synthesis of iron oxide nanoparticle using *Carica papaya* leaf extract: application for photocatalytic degradation of remazol yellow RR dye and antibacterial activity. *Heliyon* **2020**, *6*, e04603, https://doi.org/10.1016/j.heliyon.2020.e04603.
37. Xu, P.; Zeng, G.M.; Huang, D.L.; Feng, C.L.; Hu, S.; Zhao, M.H.; Lai, C.; Wei, Z.; Huang, C.; Xie, G.X.; Liu, Z.F. Use of iron oxide nanomaterials in wastewater treatment: A review. *Sci. Total Environ.* **2012**, *424*, 1-10, https://doi.org/10.1016/j.scitotenv.2012.02.023.
38. Xiao, C.; Li, H.; Zhao, Y.; Zhang, X.; Wang, X. Green synthesis of iron nanoparticle by tea extract (polyphenols) and its selective removal of cationic dyes. *J. Environ. Manage.* **2020**, *275*, 111262, https://doi.org/10.1016/j.jenvman.2020.111262.
39. Kavitha, D.; Namasivayam, C. Experimental and kinetic studies on methylene blue adsorption by coir pith carbon. *Bioresour. Technol.* **2007**, *98*, 14-21, https://doi.org/10.1016/j.biortech.2005.12.008.
40. Saha, B.; Das, S.; Saikia, J.; Das, G. Preferential and enhanced adsorption of different dyes on iron oxide nanoparticles: A comparative study. *The Journal of Physical Chemistry C* **2011**, *115*, 8024-8033, https://doi.org/10.1021/jp109258f.
41. Zhang, P.; O'Connor, D.; Wang, Y.; Jiang, L.; Xia, T.; Wang, L.; Tsang, D.C.W.; Ok, Y.S.; Hou, D. A green biochar/iron oxide composite for methylene blue removal. *J. Hazard. Mater.* **2020**, *384*, 121286, https://doi.org/10.1016/j.jhazmat.2019.121286.
42. Cheera, P.; Karlapudi, S.; Sellola, G.; Ponneri, V. A facile green synthesis of spherical Fe_3O_4 magnetic nanoparticles and their effect on degradation of methylene blue in aqueous solution. *J. Mol. Liq.* **2016**, *221*, 993-998, https://doi.org/10.1016/j.molliq.2016.06.006.